Phase Diagram for Blends of Styrene−Butadiene Diblock Copolymer and Styrene−Butadiene Random Copolymer

Hwan-Koo Lee, Dae-Cheol Kim, Seong Il Yoo, Byeong-Hyeok Sohn, and Wang-Cheol Zin*

Department of Materials Science & Engineering, and Polymer Research Institute, Pohang University of Science & Technology, Pohang 790-784, Gyeongbuk, Korea

Received January 13, 2003

ABSTRACT: The phase behaviors of the blends of diblock copolymers and random copolymers were investigated with synchrotron small-angle X-ray scattering, light scattering, differential scanning calorimetry, and transmission electron microscopy techniques. The temperature, T_{ODT}, at which the order−disorder transition (ODT) takes place, was obtained as a function of the fraction of random copolymers. The phase diagram shows three regions: homogeneous liquid phase, ordered mesophase, and a two-phase region. When the fraction of random copolymer is lower than 0.15, T_{ODT} decreases linearly as the random copolymer fraction increases. Above 0.15, the macroscopic phase separation is dominant, and T_{ODT} is nearly constant in the middle range of the fraction. We discussed phase behavior on the basis of the free energy change on mixing of a diblock copolymer and a random copolymer.

Introduction

Many studies have investigated the phase behavior of blends containing diblock copolymers. However, most of these have focused on diblock copolymer (A−B)/homopolymer (A) systems,[1−9] and some have focused on A−B/C systems[10−14] with C having a specific interaction with A. On the other hand, there have been few experimental works[15−19] on the phase behavior of diblock copolymer blends containing a copolymer (random copolymer or block copolymer), which typically exhibits different phase behavior from blend systems containing block copolymers and homopolymers.

Recently, the phase behaviors of block copolymers in solvents of varying selectivity have been extensively investigated.[20−25] In a block copolymer with a neutral solvent, the addition of a neutral solvent is analogous to increasing temperature or reduced effective interaction parameters, and the principal interdomain distance decreases on the volume fraction of solvent. A theory developed by Whitmore and Noolandi[20] predicted that there is a tendency for neutral solvents to accumulate at the microdomain interface to screen unfavorable A−B monomer contacts at the interface.

In one of our previous works,[18] we constructed a theoretical phase diagram for diblock copolymer (A−B) blends containing random copolymers (ABR) with compositions similar to those of diblock copolymers. The order−disorder transition temperature (T_{ODT}) of block copolymers was lowered by the addition of random copolymers regardless of their molecular weight. It was also found that the fraction of ABR solubilized into the A−B was very limited due to endothermic mixing between ABR and each block of A−B. An experimental study[19] on A−B/ABR blends was subsequently carried out, where the composition and the molecular weight of ABR are similar to those of A−B. We showed that the order−disorder transition temperature (T_{ODT}) and the interdomain distance (D) almost linearly decreased as the ABR fraction increased. However, the concentration of studied blends was limited up to 15 wt % of ABR, and blends containing larger amounts of ABR were not investigated in detail.

For the purpose of extending previous works and constructing an experimental phase diagram, the phase behavior of the A−B/ABR blends was studied by using small-angle X-ray scattering (SAXS), light scattering (LS), and differential scanning calorimetry (DSC) techniques. The studied diblock copolymer is poly(styrene-*b*-butadiene) containing 52 wt % styrene (S-B52), and the added random copolymer is poly(styrene-*r*-butadiene) containing 60 wt % styrene (SBR60). It is expected that, at temperatures above the T_{ODT}, the S-B52 is likely to behave as a random copolymer and that the SBR60 will be mixed homogeneously with the S-B52 due to a greatly increased mixing entropy and a much less enthalpic term compared to when SBR60 is mixed into S-B52 microdomains. On the other hand, below the T_{ODT} where S-B52 has lamellar morphology, SBR60 will have poor solubility to S-B52 due to the endothermic interaction between SBR60 and both blocks of S-B52 ($\chi_{RS} \approx \chi_{RB} \approx 0.5\chi_{SB}$). Therefore, macroscopic phase separation will occur, which will be evidenced by optical turbidity in light scattering experiments. Block copolymer-rich mesophase may reveal a periodic peak profile in SAXS experiments, since it is in a similar state to pure block copolymers. These two independent experiments, together with DSC measurements, were carried out to give complementary results on the phase behavior of S-B52 and SBR60 mixtures. Also, this experimentally obtained phase diagram is qualitatively understood by comparing the free energy of the mesophase and liquid phase.

Experimental Section

Materials. Styrene−butadiene diblock copolymer (denoted by S-B52) is the same material used in the previous study,[19] where it was designated as S-B52. It contains 52 wt % of styrene as determined by the NMR technique, and its M_n and M_w are 25 000 and 26 000, respectively. The styrene−butadiene random copolymer (denoted by SBR60) containing approximately 60 wt % styrene was kindly synthesized for our

* To whom correspondence should be addressed: Tel +82-54-279-2136; Fax +82-54-279-2399; e-mail wczin@postech.ac.kr.

10.1021/ma030020w CCC: $25.00
Published on Web 09/13/2003

use by Kumho Chemical Co., and its M_w (by LS) and M_w/M_n (by GPC) are 50 000 and 1.07, respectively.

Mixtures of samples with various random copolymer weight fractions, from 0.02 to 0.95, were prepared by the solvent-casting method. S-B52 and SBR60 were dissolved in a common solvent, toluene, at a polymer concentration less than 20 wt %. Then, an antioxidant (Irganox 1010; Ciba-Geigy Group) of 0.5 wt % was added into the solution. The solution was cast on a glass plate, and the solvent was evaporated slowly at room temperature. To remove the residual solvent, the samples were further dried under a vacuum at about 343 K for over a day. After complete removal of the solvent, the samples were further vacuum-annealed at 393 K for 24 h. The mixture sample was designated by the sample label followed by their weight percentages, as in "S-B52/SBR60 (90/10)".

Methods. a. Small-Angle X-ray Scattering (SAXS). Synchrotron SAXS measurement was performed at the 4C1 X-ray Beamline (1.608 Å in wavelength) and 1B2 Beamline (1.577 Å in wavelength) at the Pohang Accelerator Laboratory (PLS) in Korea. Scattering patterns were obtained from a diode-array position-sensitive detector (model 1412XR, EG&G Princeton Applied Research), and a beam path was maintained under a vacuum to reduce air scattering. The measured intensity was corrected for ring current decrease, background scattering, detector noise, and sample absorption. Since the optics of the SAXS equipment are point focused, the intensity was not corrected for the smearing effect by the finite cross section of the primary beam. The heating and cooling rate was fixed at 2 K/min, and the data were collected every 5 K between room temperature and the experimental limit.

b. Light Scattering (LS). The cloud temperature was determined by monitoring the intensity of scattered light at a fixed angle (~30°) through a mixture film located on a heating stage. A He−Ne laser (4 mW) was used as a light source. The scattered intensity was recorded by a photodiode detector (Newport Corp. 835 optical power meter) with a computer interface. Heating and cooling experiments were performed several times to increase the validity of the experimental results. The same heating system was used as in the SAXS experiments, which made it possible to compare the two independent data sets directly without any further corrections, such as temperature calibration, between them.

c. Differential Scanning Calorimetry (DSC). Thermal analysis was performed with a Perkin-Elmer DSC7. T_{ODT} was determined from the change of exothermic enthalpy during the cooling scan. Each sample was heated far above the melt state and then cooled to room temperature at the rate of −10 K/min.

d. Transmission Electron Microscopy (TEM). The samples were prepared by placing a drop of solution on a carbon-/Formvar-coated copper grid and letting the solvent evaporate at room temperature on a sealed glass vessel. To remove the solvent evaporation effect that may affect the observed morphology of solution-cast block copolymers, the solvent was very slowly evaporated and the samples were annealed at 35 °C for a day. To attain equilibrium morphology, the samples were further annealed above the glass transition temperatures of both blocks in a vacuum oven for 5 h. The samples were then exposed to the vapor of a 2% aqueous OsO_4 solution. OsO_4 is a selective staining agent for the butadiene blocks. TEM was performed on a JEOL 1200EX electron microscope operated at 120 kV.

Results and Discussion

The microscopic phase behavior of the mixture was examined using the SAXS method to investigate the effect of added SBR60 on the stabilization of the S-B52 microdomain structure. The scattered X-ray intensity data were obtained with S-B52/SBR60 having various SBR60 weight fractions from 0 to 0.95. From the plot of the scattered X-ray intensity against the scattering vector q ($4\pi\lambda^{-1}\sin\theta$) in the low-temperature region (strong segregation regime), first, third, and fifth Bragg peaks for S-B52 appeared at q = 0.29, 0.88, and 1.45 nm^{-1}. Thus, the ordered morphology of S-B52 is lamellar as evidenced by the ratios of the peak scattering vectors. The first peak ($D = 2\pi/q^*$) corresponds to a lamellar interdomain spacing of 22.5 nm. On the basis of discontinuity in the I_m^{-1} vs T^{-1} plots, the T_{ODT} of S-B52 was found to be 459 K.

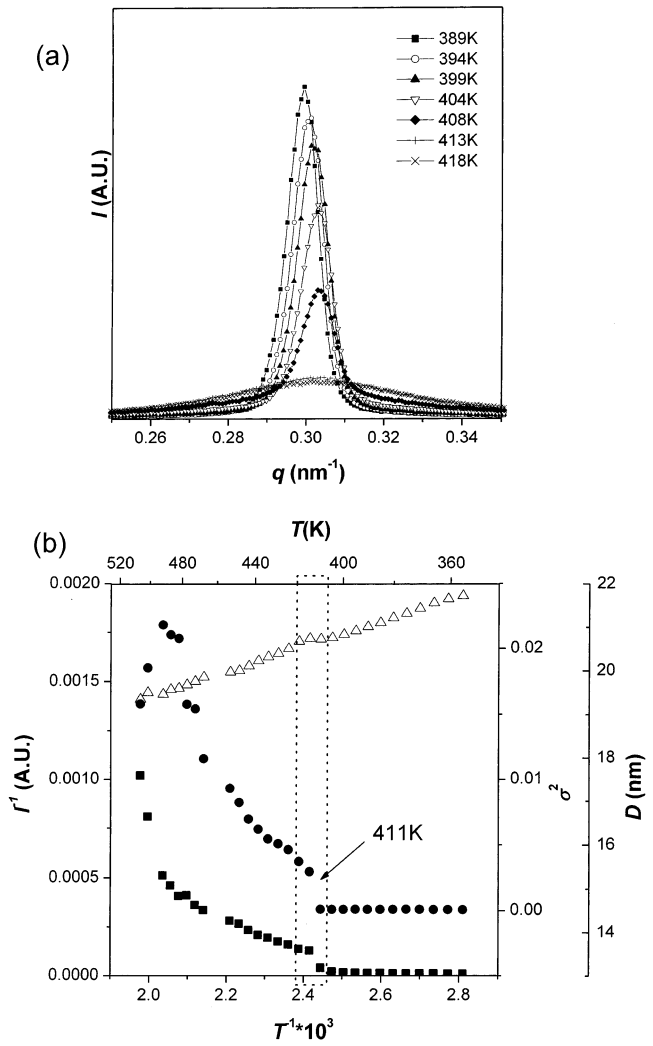

Figure 1. (a) SAXS intensity of S-B52/SBR60 (80/20) as a function of temperature. T_{SAXS} = 411 K, at which abrupt falling of the intensity with increasing temperature is clearly seen. (b) Plots of I_m^{-1} (■) vs T^{-1}, σ^2 (●) vs T^{-1}, and D (△) vs T. The discontinuity of each plot appears at the same temperature marked by the dotted box (411 K).

Figure 1a displays the scattered primary X-ray intensity profiles of S-B52/SBR60 (80/20) near the T_{ODT} on cooling. A sharp change of the profiles at temperatures between 399 and 413 K is clearly observed. The ODT temperature can be determined from this discontinuous change in the SAXS profile.[26,27] The narrow peak obtained below the T_{ODT} is the first Bragg reflection of the lamellar microdomain periodic structure. After an abrupt intensity drop at 413 K, the intensity is continuously reduced by raising the temperature. The remnants of the peaks that persist to the highest temperature are due to the concentration inhomogeneity present even in a thermodynamically homogeneous polymer melt, stemming from the so-called correlation hole effect.[28] Repulsive interactions between styrene and butadiene drive local physical clustering of similar segments, and this process results in a finite size

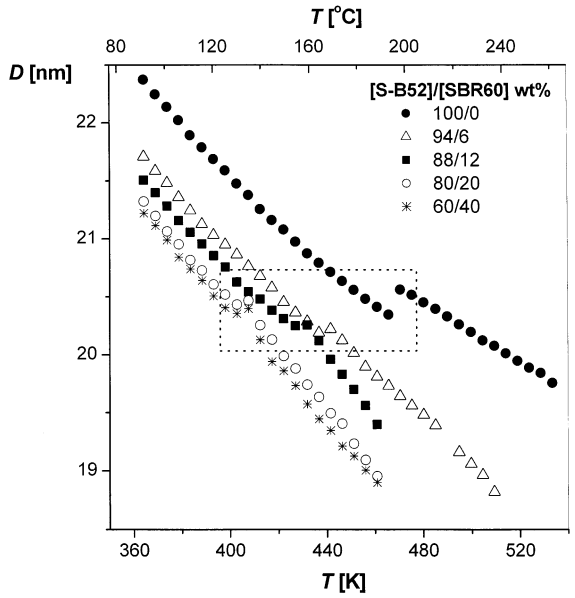

Figure 2. Temperature dependence of interdomain distance (D). D is determined from the scattering vector q^* at the first-order scattering maximum.

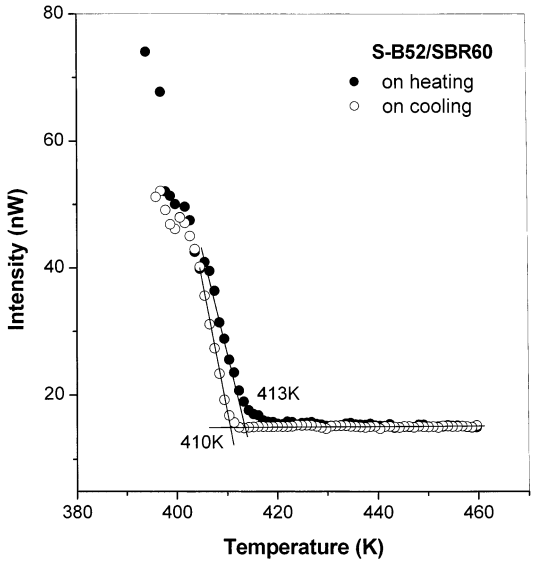

Figure 3. LS results for S-B52/SBR60 (80/20) where reproducibility of the results is clearly seen. The T_{LS} for S-B52/SBR60 (80/20) is 413 K (heating) and 410 K (cooling).

stabilization of the disordered state on the microdomain length scale.[29] As for other mixtures, a phenomenon similar to the mixture of (80/20) is obtained.

Figure 1b shows the three plots of I_m^{-1} vs T^{-1}, σ^2 vs T^{-1}, and D vs T all together for S-B52/SBR60 (80/20) on cooling. Here, I_m indicates the maximum intensity of the primary peak and σ^2 the square of the half-width at half-maximum of the primary peak. D ($=2\pi/q^*$) is determined from the scattering vector q^* at the first-order scattering maximum. It is clearly seen that the abrupt increase of σ^2 or I_m^{-1} with decreasing T^{-1} occurs almost at the same temperature. This specific temperature is denoted by T_{SAXS}. The steady diminution of D upon increasing T corresponds to the shift of the peak position toward higher q value in Figure 1a, which is due to chain shrinkage to a Gaussian coil arising from an increase in entropy on mixing. We observed that D increases slightly upon raising the temperature across T_{SAXS} and that this discontinuity in D is expected since ODT is a weak first-order transition.[30] In a disordered state, D corresponds to the spatial extent of concentration fluctuations, which are activated by thermal energy, whereas in the ordered state, it corresponds to the spacing for lamellar microdomain structures generated by block segregation. As for other mixtures, a similar plot to Figure 1b is obtained.

The change in lamellar interdomain distance (D) with temperature is shown in Figure 2. D slightly decreases on the addition of SBR60 within the whole temperature range. The decrease of the microdomain spacing of diblock copolymers due to the addition of homopolymers was already reported by Winey et al.[6] However, the decrement of D as shown in Figure 2 occurs when a random copolymer of higher molecular weight (50K) is added into the S-B52 (26K). This phenomenon can be explained by considering the localization of SBR60 in the interfacial region of S-B52 microdomain. Unlike the selective homopolymers that are localized into either the S- or B-domain, causing axial microdomain size to increase, SBR60 might dissolve in the interfacial region of the S-B52 lamellar domain with a simple density distribution centered at the interface since it has poor solubility to both S- and B-domain of S-B52. The addition of SBR60 induces expansion of the junction points at the interface to increase S-B52 lateral microdomain size. Thus, added SBR60 induces slight axial contraction in S-B52 microdomain structure. However, it should be noted that macroscopic phase separation occurs above the solubility limit of SBR60 (about 15 wt %) and that the D does not change noticeably, as seen in Figure 2.

The macroscopic phase behavior of the blends of S-B52 and SBR60 was investigated using the light scattering (LS) technique. Experimental results for S-B52/SBR60 (80/20) are shown in Figure 3, in which the scattered intensity at low temperatures decreases with increasing temperature up to a certain temperature (denoted by T_{LS}), and from there on, the intensity remains fairly steady at a low value to the experimental limit, which indicates that as the temperature rises, macroscopically phase-separated blend turns homogeneous. T_{LS} determined for S-B52/SBR60 (80/20) is 413 K on heating and 410 K on cooling, with a difference of 3 K between them. This macroscopic phase separation is observed in the concentration range from (85/15) to (12/88); this region will be denoted as "M + L" in the phase diagram, "M" being a mesophase rich in S-B52 where the ordered microdomain structure of S-B52 is mixed with a small amount of SBR60 and "L" being a liquid phase where S-B52 and SBR60 are mixed homogeneously in a disordered state. The phrase "rich in" is used since there is a possibility of a very small amount of SBR60 being mixed with the S-B52 in an ordered state because of the infinite driving force to stabilize mesophase on mixing at $\phi_{SBR60} = 0$, arising from the entropic term. We should note that the transition from the "M + L" phase to the "L" phase observed in the LS experiment has been also detected by the SAXS experiment in terms of the order−disorder transition because the transition from the M + L phase to the L phase implies the disappearance of the M phase, i.e., the microdomain structure. However, there is a difference in the dimension of examination between them. The former detects a microscopic change of microdomain structure in block copolymers, and the latter examines

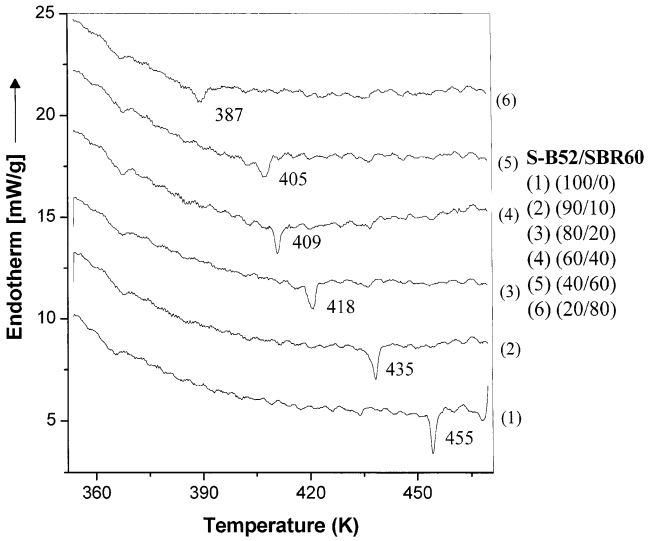

Figure 4. DSC traces (−10 K/min) recorded during the first cooling scan. The T_{DSC} decreases as the SBR60 fraction increases. The cooling curves have been shifted vertically for clarity.

large-scale changes such as macroscopic phase separation.

The DSC cooling traces of mixtures are seen in Figure 4. Although the change in heat on ODT is minute, we can see an exothermic enthalpy change, which indicates a weak first-order transition from a disordered phase to an ordered mesophase (denoted by T_{DSC}). Exothermic heat changes can be found over all concentration ranges, since there is always a microscopic phase transition between mesophase and liquid phase. The T_{DSC} gradually decreases as the fraction of SBR60 increases. We see that, in the region where the SBR60 weight fraction lies between 0.4 and 0.6, the depression of T_{DSC} is very weak. This region will be discussed later together with T_{LS} from LS experiments.

The electron micrographs of blends containing 10 and 20 wt % of SBR60 are shown in Figure 5a,b. Each of these images is a representative one selected from a much broader area that we investigated. A blend containing 10 wt % of SBR60 forms S-B52 lamellar microdomain structures mixed with a small amount of SBR60, and that containing 20 wt % of SBR60 forms both lamellar microdomains and macroscopically phase-separated domains of SBR60. Lamellar microdomains rich in S-B52 are composed of alternating lamellae of styrene and butadiene microdomains corresponding to the equilibrium morphology of neat S-B52. Because of selective staining, butadiene domains appear dark and styrene domains bright in the lamellar microphase of blends in the TEM micrograph. The macroscopically phase-separated domains appear gray because SBR60 contains both styrene and butadiene throughout the domains. As shown in Figure 5b, the ordered "M" phase rich in S-B52 and the disordered "L" phase rich in SBR60 coexist in a macroscopically phase separated "M + L".

In Figure 6 the transition temperatures obtained with the SAXS, LS, and DSC experiments are plotted as a function of the weight fraction of SBR60. The "L" phase above the transition line indicates the homogeneous mixed phase of S-B52 and SBR60 in the disordered state. The "M" phase below the transition line indicates the ordered microdomain structure of S-B52 mixed with

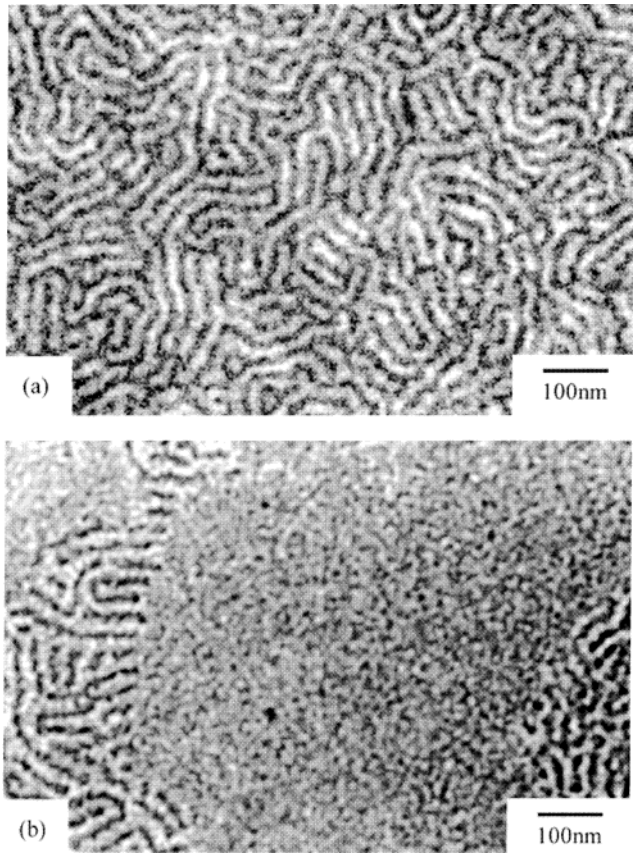

Figure 5. TEM images of S-B52/SBR60 blends at various SBR60 concentrations: (a) blend containing 10 wt % SBR60, (b) blend containing 20 wt % SBR60. Butadiene blocks were selectively stained with OsO_4 and appeared as dark regions.

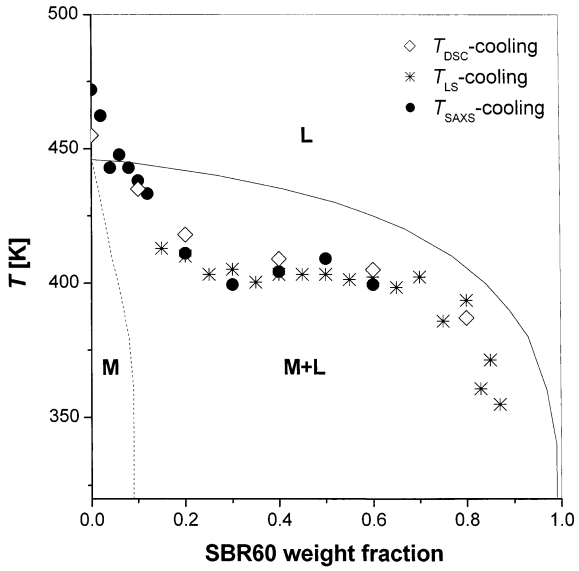

Figure 6. Phase diagram obtained from the SAXS, DSC, and LS studies on S-B52/SBR60. Listed symbols are T_{SAXS} cooling (●), T_{LS} cooling (∗), and T_{DSC} cooling (◇). These independent experiments show a good agreement with each other. The solid line denotes the calculated phase boundary from "M + L" to "L", and the dashed line is the phase boundary from "M" to "M + L" drawn as a guide to the eye.

SBR60. T_{SAXS} shows a two-step dependency on the weight fraction of SBR60: in the region where SBR60 weight fraction is lower than 0.15, the T_{SAXS} shows a prominent depression, and then the T_{SAXS} shows little

dependency. A macroscopic phase transition from "M" to "M + L" occurs above the solubility limit (SBR60 weight fraction ~ 0.15). The depression of the T_{ODT} in the region where SBR60 weight fraction is larger than 0.15 can be explained by considering the melting point depression occurring in polymer/good solvent systems. In this region, there are two macrophases consisting of an ordered phase and a disordered one. The ordered phase is comprised of S-B52 microstructures mixed with a small amount of SBR60 in the interface, and the disordered phase is comprised of SBR60 containing a small amount of S-B52. There are two differences between S-B52/SBR60 and common crystal/solvent systems: (1) An increase in mixing entropy of added random copolymer is less than that of added solvent, and (2) there is slight random copolymer solubilization in the formation of mesophase. It should be noted that since SBR60 has poor solubility to either the S- or B-domain of S-B52, we take into account the mixing of the added SBR60 in the interfacial region of the microdomain structure of S-B52. Therefore, a very small amount of added SBR60 might be dissolved into the microdomains of S-B52, and there is only an ordered phase "M" comprised of S-B52 mixed with a small amount of SBR60 within the S-B52 interface.

We should note that the results of the LS experiments show a good correspondence with those of the SAXS experiments. The T_{LS} decreases gradually with increases in SBR60 weight fraction. Optical transparence in the region where the SBR60 weight fraction is lower than 0.15 means that there is one phase, not two macroscopically separated states. The T_{LS} drop in the region where SBR60 weight fraction is larger than 0.7 is similar to the melting point depression on crystal/solvent systems as discussed above. On the basis of the phase diagram, there is a very small amount of "M" phase in this region, resulting in the disappearance of the Bragg reflection peaks in the SAXS experiments. Thus, we cannot investigate the order−disorder transition by using the SAXS method. As seen in Figure 6, however, by using the LS method, the macroscopic phase separation transition between "L" and "M + L" phases can be examined in this region. This means that a macroscopically phase-separated state, "M + L", remains below that transition line, even though the S-B52-rich phase loses its long-range order.

To explain this drop of the T_{LS}, the free energy change of the mesophase "M" can be compared to that of disordered liquid phase "L" at various temperatures. In previous work by Lee et al.,[18] a phase diagram was constructed for A−B/ABR blends by the modified confined-chain model developed earlier. However, the above paper assumed that contributions to the free energy caused by the solubilization of random copolymer in the interfacial regions between microdomains are small and can be neglected. To define a reference state, the free energy of a disordered state formed by pure SBR60 and that of an ordered state formed by pure S-B52 are set to zero. The free energy change from an ordered to a disordered state of pure block copolymer, ΔG_{mst}, can be expressed as follows:

$$\Delta G_{mst} = \Delta H_{mst} - T\Delta S_{mst}$$

It has a positive value below the T_{ODT}, and as the temperature is raised, it gradually decreases in magnitude and eventually becomes zero at the T_{ODT} of the block copolymer. Then the free energy change of liquid

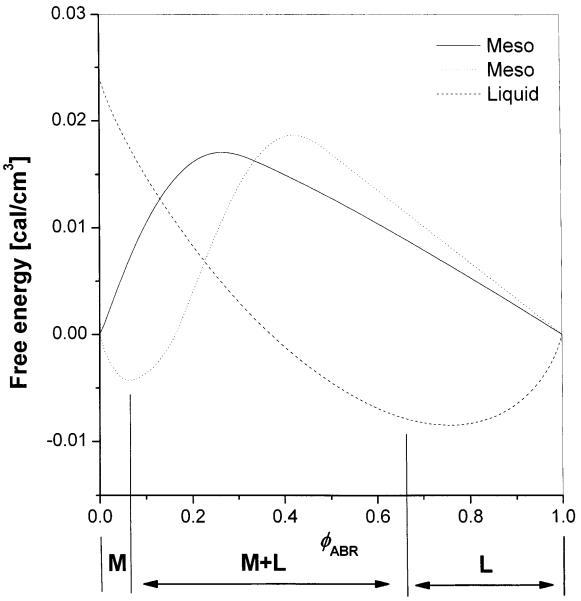

Figure 7. Example for determining coexistent phase using the tangent line method with the expected free energy changes of "M" and "L" phase at a given temperature. The free energy change of "M" phase is expressed by a solid line and that of the "L" phase by a dashed line. The dotted line is the free energy change of "M" phase, considering the solubilization of random copolymer in the interfacial region.

phase in a blend of S-B52 and SBR60 is given by

$$\Delta G_{liq} = \Delta G_{random} + \Delta G_{mst}\phi_{A-B}$$

where ΔG_{random} is the free energy change of mixing of a random copolymer with a disordered block copolymer and is estimated by the Flory−Huggins equation.

$$\Delta G_{random} = [(\phi_{A-B}/V_{A-B}) \ln \phi_{A-B} + (\phi_{ABR}/V_{ABR}) \ln \phi_{ABR}] + B_{A-B/ABR}\phi_{ABR}\phi_{A-B}$$

with

$$B_{A-B/ABR} = (f_A - f_A')^2 B_{A/B}$$

Here, ϕ_{ABR} and ϕ_{A-B} are the volume fractions of the two polymers. $B_{A/B}$ is the interaction energy density between A and B, and f_A and f_A' are the fractions of component A in the block copolymer and the random copolymer, respectively. V_{A-B} and V_{ABR} are the molar volumes of two copolymers. The free energy changes of mesophase on mixing of random copolymer (ΔG_{meso}) were estimated by the use of a modified confined chain model incorporating some reasonable assumptions on mixing entropy.[18]

The calculated phase boundary, based on the previous theory,[18] is also shown as solid line in Figure 6. In contrast to the experimental results, the temperature at which the phase transition from "M + L" to "L" takes place gradually decreases as the weight fraction of SBR60 increases. The dashed line is the phase boundary from "M" to "M + L" drawn as a guide to the eye. The mesophase M exists only over a narrow concentration range below the T_{ODT} of pure S-B52.

Figure 7 is plotted as an example for determining coexistent phases under a given temperature. The coexisting "M + L" phase is determined graphically by constructing a common tangent line. To simplify the calculation of the mesophase free energy change, it is

assumed that the densities of A and B polymers are both 1 g/cm^3, allowing $M_K = V_K$ (K = A and B). For the interaction energy density $B_{A/B}$, we used the experimental value for the polystyrene−polybutadiene pair determined in previous work[31]

$$B_{A-B} = 1.6 - 0.002T \quad (\text{cal/cm}^3)$$

where T is the temperature in kelvin. The molecular parameters used in this figure are as follows: $M_{A-B} =$ 25 000, $M_{ABR} =$ 46 730, $f_A = 0.52$, $f_A' = 0.6$, and $T =$ 420 K. As seen in Figure 7, the free energy change of the mesophase increases rapidly, indicating that the mesophase of S-B52 containing a small amount of SBR60 is unstable. Since this theory assumes that added SBR60 can be solubilized either into the S domain or the B domain, SBR60 is hardly dissolved into the microdomain of S-B52 due to the increased mixing enthalpy. That is, macroscopic phase separation occurs when the SBR60 is added to S-B52. However, if we consider the solubilization of random copolymer in the interfacial regions in microdomains as figured by gradual reduction of D below the weight fraction of 0.15, the increase of enthalpic energy on solubilization will be negligibly small since the composition of SBR60 is very close to that in the interfacial region of the microdomain. Even though the entropy gain of random copolymers solubilized in the interfacial region may not be large, the free energy change of mesophase may be lowered when a small amount of SBR60 is added to S-B52. The expected free energy curve of mesophase, considering the possibility of solubilization of random copolymer in the interfacial region and the experimentally obtained phase diagram, is schematically plotted as a dotted line in Figure 7. At this stage, we cannot compare the experimental data with theory of more realistic models, including the solubilization of random copolymers in the interface.

Conclusions

On the basis of SAXS, LS, DSC, and TEM studies, the order−disorder transition temperature of S-B52/SBR60 blend, T_{ODT}, was found to show two-step behavior by increasing the weight fraction of random copolymers. In the region where the SBR60 weight fraction is lower than ≤0.15, the mesophase was formed by solubilization of random copolymers into the interface of the block copolymer microdomain. In macroscopically phase-separated regions, the depression of T_{ODT} behaves like a melting point depression. These three independent experiments complement each other and provide the information to construct phase diagrams for S-B52/SBR60 blend systems, as shown in Figure 6. The phase diagram has three regions: two homogeneous phases, "M" and "L", and one inhomogeneous phase, "M + L". The "M + L" phase below the transition line indicates that the ordered "M" phase rich in S-B52 and the disordered "L" phase rich in SBR60 coexist in a macroscopically phase-separated state.

Acknowledgment. This work was supported by the Korea Research Foundation (KRF-2002-005-D00009). The assistance of the Pohang Accelerator Laboratory in performing SAXS measurements is gratefully acknowledged.

References and Notes

(1) Zin, W.-C.; Roe, R.-J. *Macromolecules* **1984**, *17*, 183.
(2) Roe, R.-J.; Zin, W.-C. *Macromolecules* **1984**, *17*, 189.
(3) Kang, C.-K.; Zin, W.-C. *Macromolecules* **1992**, *25*, 3039.
(4) Matsen, M. W. *Macromolecules* **1995**, *28*, 5765.
(5) Whitmore, M. D.; Noolandi, J. *Macromolecules* **1985**, *18*, 2846.
(6) Winey, K. I.; Thomas, E. L.; Fetters, L. J. *Macromolecules* **1991**, *24*, 6182.
(7) Nojima, S.; Roe, R.-J. *Macromolecules* **1987**, *20*, 1866.
(8) Tanaka, H.; Hasegawa, H.; Hashimoto, T. *Macromolecules* **1991**, *24*, 240.
(9) Baek, D. M.; Han, C. D.; Kim, J. K. *Polymer* **1992**, *33*, 4821.
(10) Tucker, P. S.; Barlow, J. W.; Paul, D. R. *Macromolecules* **1988**, *21*, 1678.
(11) Tucker, P. S.; Barlow, J. W.; Paul, D. R. *Macromolecules* **1988**, *21*, 2794.
(12) Tucker, P. S.; Paul, D. R. *Macromolecules* **1988**, *21*, 2801.
(13) Hashimoto, T.; Kimishima, T.; Hasegawa, H. *Macromolecules* **1991**, *24*, 5704.
(14) Lee, H.-K.; Kang, C.-K.; Zin, W.-C. *Polymer* **1996**, *37*, 287.
(15) Cifra, P.; Karasz, F. E.; MacKnight, W. J. *Macromolecules* **1989**, *22*, 3649.
(16) Shi, A.-C.; Noolandi, J.; Hoffmann, H. *Macromolecules* **1994**, *27*, 6661.
(17) Kim, J. K. *Polymer* **1995**, *36*, 1243.
(18) Lee, H.-K.; Zin, W.-C. *Macromolecules* **2000**, *33*, 2894.
(19) Kim, D.-C.; Lee, H.-K.; Sohn, B.-H.; Zin, W.-C. *Macromolecules* **2001**, *34*, 7767.
(20) Whitmore, M. D.; Noolandi, J. *J. Chem. Phys.* **1990**, *93*, 2946.
(21) Hong, K. M.; Noolandi, J. *Macromolecules* **1983**, *16*, 1083.
(22) Fredrickson, G. H.; Leibler, L. *Macromolecules* **1989**, *22*, 1238.
(23) de la Cruz, M. O. *J. Chem. Phys.* **1989**, *90*, 1995.
(24) Lodge, T. P.; Hamersky, M. W.; Hanley, K. J.; Huang, C. I. *Macromolecules* **1997**, *30*, 6139.
(25) Hanley, K. J.; Lodge, T. P.; Huang, C. I. *Macromolecules* **2000**, *33*, 5918.
(26) Ogawa, T.; Sakamoto, N.; Hashimoto, T.; Han, C. D.; Baek, D. M. *Macromolecules* **1996**, *29*, 2113.
(27) Tanaka, H.; Hashimoto, T. *Macromolecules* **1991**, *24*, 5713.
(28) Bates, F. S. *Macromolecules* **1985**, *18*, 525.
(29) Guenza, M.; Schweizer, K. S. *J. Chem. Phys.* **1997**, *106*, 7391.
(30) Fredrickson, G. H.; Helfand, E. *J. Chem. Phys.* **1987**, *87*, 697.
(31) Roe, R.-J.; Zin, W.-C. *Macromolecules* **1980**, *13*, 1221.

MA030020W